15

Stand for testing extreme ultraviolet sensitive photoresists

© A.Ya. Lopatin, V.I. Luchin, A.N. Nechay, A.A. Perekalov, A.E. Pestov, D.G. Reunov, N.I. Chkhalo

Institute for physics of microstructure RAS,
603087 Afonino, Kstovo district, Nizhny Novgorod, Russia
e-mail: aepestov@ipm.sci-nnov.ru, lopatin@ipmras.ru

Received April 26, 2024
Revised April 26, 2024
Accepted April 26, 2024

An experimental stand for testing photoresists sensitive to extreme ultraviolet radiation is described. The stand is based on a laser-plasma source with a Nd:YAG-laser (pulse energy 0.8 J, pulse duration 5.2 ns, focal spot diameter 66 μm, peak intensity up to $3 \cdot 10^{12}$ W/cm^2) and a gas jet as a target, as well as a mirror monochromator (a replaceable multilayer X-ray mirror optimized for a selected wavelength). The setup is equipped with a set of mirrors and filters for exposing samples at wavelengths of 11.2, 13.9 and 30.4 nm. Kr, Ar and He are used as working gases, the ions of which Kr X, Ar VIII and He II have intense emission bands in the vicinity of the indicated wavelengths. The stand was tested with photoresist samples, the size and shape of the focal spot were determined, which was about 0.5×1.0 mm^2.

Keywords: multilayer x-ray mirrors, monochromator, collector, x-ray and extreme ultraviolet wavelength range, photoresist, EUV lithography.

DOI: 10.61011/TP.2024.08.59010.142-24

Introduction

Currently, projection nanolithography at a wavelength of 13.5nm has become a key technology used in the manufacture of critical layers of ultra-large integrated circuits according to nanometer technological standards [1–3]. In particular, the latest generation installation from ASML (TWINSCAN NXE:3400B), operating in the extreme ultraviolet (EUV) range at a wavelength of 13.5 nm, has a capacity of up to 150 plates with a diameter of Ø 300 mm per hour and provides a spatial resolution of 13 nm [4,5].

The possibility of reducing technological limits to a level of less than 10 nm involves the use of double patterning which doubles the number of process operations and, accordingly, reduces the productivity of the lithographic process. Attempts to avoid the double patterning by increasing the numerical aperture of the projection lens have encountered both technological problems in the manufacture of high-power lenses and the fundamental problem associated with shading on the mask. Since masks for EUV lithography have a three-dimensional topology, at large illumination angles, the effects of shading the mask pattern appear, which do not allow obtaining high-quality images. ZEISS offers a unique lens with different magnifications ($4\times$ and $8\times$) in perpendicular planes for solving this problem [6]. The first experimental lithograph with a numerical aperture $NA = 0.55$ and an estimated resolution of 9 nm was shipped to Intel at the end of 2023. However, there have been no reports of the success of this technology so far.

The shortening the operating wavelength is another technique that allows increasing the spatial resolution and productivity of the process. In this case, it is possible to use already well-proven projection lenses with a numerical aperture $NA \sim 0.3$. The authors proposed using the wavelength range 6.6 nm for these purposes in Ref. [7]. *K*-edge of boron absorption lies in this region, and multilayer mirrors La/B and U/B have the highest reflection coefficients, mirrors Sb/B4C have good stability of the reflection coefficient [8]. Research has been conducted since the end of 2008 in the field of X-ray sources [9], optics [10,11], photoresists for the so-called BEUV (beyond EUV) lithography [12]. The authors summarized the results of five years of research in Ref. [13] and convincingly showed that even subsequent developments would not lead to sufficient productivity for mass production. It will be inferior in 20−30 times to lithography at a wavelength of 13.5 nm. However, the same article shows that the performance in the area of 11 nm will be comparable to lithography at 13.5 nm, or even one and a half times higher. At the same time, the resolution will increase by 20−25%.

The Russian Federation also conducts studies for the creation of its own technology for short-wave lithography. Various wavelengths are considered promising, including 13.5 and 11.2 nm [3.14], as well as shorter wavelengths [15.16]. There are projects for creation of a maskless EUV nanolithograph [17].

The development of high-resolution photoresists is one of the priorities of research conducted in the field of micro- and nanolithography. For instance, significant resources are allocated for solving this problem in relation to lithography with an operating wavelength of 248 nm, and experimental batches of a number of photopolymers sensitive at this wavelength with a spatial resolution no worse than 0.14 μm should be produced by the end of 2025, as their industrial production should be prepared and launched [18].

It would be logical to expect the availability in a comparable time of the fundamental component of the modern lithographic system which is a projection lens providing an equally high level of spatial resolution with an acceptable field of view size for microelectronic production. The characterization of the lens should not be conditioned by the presence of appropriate resist, since it can be performed without their use. For example, a direct experimental evaluation of the point scattering function using a transparent mask, which is a set of calibrated microholes, may, in our opinion, be significantly more informative and minimize the ambiguity of interpretation of the results by the projection optics testing methodology.

It is also possible to estimate the resolution without using resist for EUV lenses developed at the IPM RAS for lithographic schemes of the EUV spectral range [17]. The IPM's instrument base of electronic lithography and microscopy, surface ion etching, developed approaches to fabrication of metal membranes with a thickness of $0.1\,\mu$m and less — all this together allows counting on the successful production of systems of holes of substantially submicron sizes on thin-film membranes. It should be noted that the capabilities of the projection systems of the EUV range are many times higher in terms of design resolution than the capabilities of optics operating at the long-wavelength edge of the UV spectrum. Even in a simple two-mirror system with axisymmetric asphericization of mirrors, it is possible to achieve a resolution of 27 nm in a field with a diameter of about 1.4 cm with a reduction factor of $10\times$ and operating at a wavelength of 13 nm [19]. And although the dimensions of the mentioned system (diameter of a large mirror 50 cm) are still quite large from the point of view of the current level of development for the Russian Federation in the manufacture of precision optics, the introduction of EUV range lithographs into the industry seems inevitable over time. The certification of photoresists sensitive in this part of the spectrum is one of the important aspects of such a transition.

A series of projects has been successfully completed at the IPM RAS for the study of a number of double and triple copolymers of polymethylmethacrylate (PMMA) synthesized at Research Institute for Chemistry of Nizhny Novgorod Lobachevsky University as photoresists sensitive in the EUV range [20]. According to the test results, the most sensitive photoresist compositions at this wavelength were selected in a scheme with a laser-plasma source of exposing EUV radiation and multilayer mirrors concentrating radiation at a wavelength of 13.5 nm. An important practical problem was solved using one of the developed resist — photographing of the source in the EUV region and determining its size at a wavelength of 13.5 nm ($50 \times 80\,\mu$m) and a series of photographs was used to reconstruct the brightness distribution along transverse coordinates at this wavelength [21]. These studies were continued in papers [22,23].

Currently, studies are underway at IOMC RAS for the development of chemically enhanced photosensitive polymers based on organometallics, which requires research on their sensitivity and radiation resist both at the operating wavelength and in a wider range of short-wave radiation.

This paper describes an easy-to-use laboratory test bench for the study of photopolymers sensitive to EUV radiation. The test bench implements the simplest optical circuit, which is based on the use of a spherical mirror in the geometry of the incidence of radiation close to normal, with the placement of the object and image on the Rowland circle associated with the mirror, or in its immediate vicinity. At the same time, the condition of minimization of aberrations is fulfilled [24]. The working wavelength of the radiation can be quickly replaced by changing the working gas of the laser-plasma source and the monochromator mirror with a multilayer interference coating.

1. Description of the test bench

During the development of the test bench, a concept using a laser-plasma source was chosen, which allows obtaining high intensity in a wide range of wavelengths from vacuum ultraviolet to soft X-rays. A jet of gas flowing from a nozzle is used as a target of a laser-plasma source. Much slower contamination of X-ray optical elements is the advantage of such a source compared to a source with a solid-state target. By choosing different gases and gas mixtures, the source spectrum can be coordinated to a certain extent with the operating wavelength of the multilayer mirror collecting radiation on the exposed sample. The characteristics of the Nd:YAG laser used (pulse energy 0.8 J, pulse duration 5.2 ns, focus spot diameter $66\,\mu$m, peak intensity up to $3 \cdot 10^{12}$ W/cm^2) allow plasma to be heated to temperatures at which spectral lines in the shortwave part of the EUV range are also effectively radiated. In particular, ion lines C V with wavelengths 3.6 and 4.1 nm were confidently recorded for carbon-containing targets [25]. The image and diagram of the experimental photoresist test bench are shown in Fig. 1.

Apparently, the test bench is built on the basis of a vacuum chamber with a capacity of about 75 L (a cylinder with a diameter of 150 mm and a height of 430 mm). The chamber has four connecting flanges including two flanges occupied by optical inputs, one reserved flange and one designed for loading experimental samples. Laser radiation is introduced into the vacuum chamber through a transparent window, the second window is used for visual inspection (presence of a spark, sample movement, etc.). The vacuum pumping station is a two-stage system consisting of a pre-vacuum and turbomolecular pumps; pressure control is carried out using a dual-band vacuum meter and a pair of vacuum sensors — PMT-10 and PMM-32.

The principle of operation of the test bench is as follows. The radiation of Nd:YAG laser *1* with a wavelength of 1064 nm and a pulse repetition rate of 1–10 Hz (set by a pulse generator for a specific task) using a short-focus lens

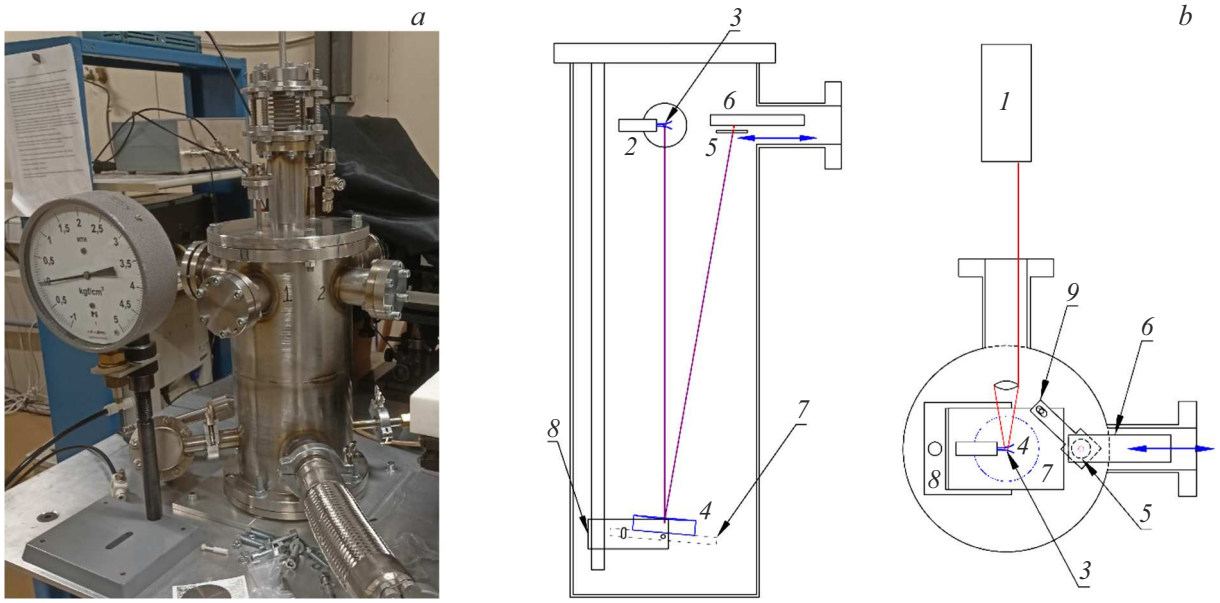

Figure 1. Photo (*a*) and diagram (*b*) of the experimental test bench (side view and top view): *1* — Nd:YAG laser, *2* — pulsed gas nozzle, *3* — laser plasma, *4* — multilayer EUV mirror, *5* — EUV radiation filter, *6* — photopolymer sample mounted on a linear translator, *7* — monochromator mirror mounting platform, *8* — frame-holder of the monochromator mirror mounting platform, *9* — EUV radiation filter holder.

focuses on a gas jet coming from a pulse nozzle *2*; the pulse repetition rate of the laser is synchronized with the opening frequency of the nozzle valve. The pulse nozzle is used to facilitate the pumping of gas from the vacuum volume, which allows pumping with a relatively low-performance turbomolecular pump with a pumping speed of 1000 L/s. When laser radiation interacts with gas atoms, multiple ionization occurs, followed by recombination radiation of multicharged ions from the laser plasma *3*. The radiation emitted in $4\pi\ sr$ is collected and monochromatized (using a multilayer Bragg mirror deposited on the surface) by a concave spherical multilayer collector mirror monochromator *4* mounted at an angle 5° to the axis of incident radiation, and passing through thin-film absorption filter *5*, focuses on a plate with a photopolymer *6* mounted on a linear translator. A thin-film absorption filter passes radiation with an operating wavelength and cuts off background visible and ultraviolet radiation contained in the laser plasma radiation spectrum. Several points with different radiation doses can be formed on a plate with a photopolymer in one pumping of the vacuum system by moving the sample using a linear translator.

2. Test bench alignment

The test bench is aligned by a visible light, using a white LED in a surface-mounted housing (smd) of standard size 0805. The LED is centered on a sleeve that fits tightly onto the tip of the pulsed gas nozzle in such a way that the light source with an accuracy of ± 0.1 mm coincides with the position of the laser-plasma source. The multilayer mirror is mounted on a movable monochromator mirror mounting platform *7*, capable of moving along the rack. In this case, it is possible to change the position of the radiation source (laser plasma) and its image relative to the Rowland circle associated with the multilayer mirror. In addition, the platform can be tilted relative to the horizontal axis so that the angle of incidence of the central beam on the mirror can be changed within small limits. Such movements make it easy to adjust the reflected beam to the center of the sample and achieve a minimum size of the focus spot. After adjusting the position of the monochromator mirror, the screws are tightened that fix the position of the platform on the rack and the tilt of the platform relative to the frame-holder of the monochromator mirror mounting platform *8*. Then, an EUV radiation filter *5* is installed in front of the sample, the holder of which *9* also allows it to be shifted in two directions, due to which it is possible to install the filter in such a way that the central beam reflected from the mirror passes through the center of the filter aperture.

3. X-ray optical elements of the test bench

To date, the test bench is provided with sets of spherical Bragg mirrors (radius of curvature $R = 320$ mm) and film filters for wavelengths of 11.2, 13.9 and 30.4 nm.

A multilayer Mo/Be structure with a period of 5.8 nm and the number of bilayers $N = 80$ was selected for a wavelength of 11.2 nm. The structure was fabricated on a quartz spherical substrate by magnetron sputtering on an installation described in detail in Ref. [26]. Structures with a

period gradient over the surface were applied, providing the best reflection at the central angle of incidence of radiation $\theta_i = 5°$. Spectral dependences of the reflection coefficient for two points (in the center of the mirror and at the edge of the aperture), measured using a laboratory reflectometer based on a monochromator spectrometer constructed according to the Czerny–Turner configuration, and a solid-state (stainless steel) laser plasma source target [27], are shown in Fig. 2.

Apparently, there is a good coincidence of the spectral reflection curves. The peak values of the reflection coefficient were $R = 69.3$ and 67.8% for points $r = 0$ and 20 mm, respectively.

A Mo/Si structure with a period of 6.9 nm and a number of bilayers $N = 50$ was synthesized for operation at a wavelength of 13.9 nm. The spectral dependences of the reflection coefficient for this mirror are shown in Fig. 3. The peak values of the reflection coefficient were $R = 60.5$ and 58.0% for points $r = 0$ and 20 mm, respectively.

A Mo/Si structure with a period of 15.8 nm and a number of bilayers $N = 15$ was synthesized for operation at a wavelength of 30.4 nm. Angular dependences of the reflection coefficient taken at a fixed wavelength of 30.4 nm (He II ion radiation) on a specialized reflectometer with a gas discharge source [28], shown in Fig. 4. The peak values of the reflection coefficient were $R = 18.8$ and 19.2% for points $r = 0$ and 20 mm, respectively.

Thus, highly reflective multilayer structures were synthesized, optimized for promising lithographic wavelengths, as well as the wavelength of the He II ion radiation, which is of interest in studies, in particular, of the solar corona [29,30].

Filters — films of submicron thickness are necessary to block long-wave radiation reflected nonresonantly by a mirror. In our case, a Be film with a thickness of $d = 200$ nm was used for operation at all wavelengths. The calculated spectral dependence of the transmission coefficient of the

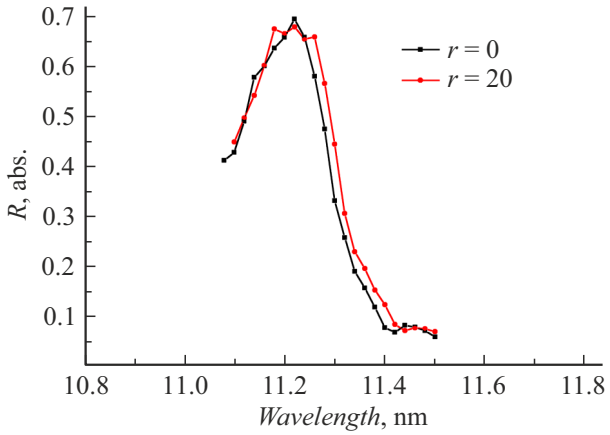

Figure 2. Spectral dependences of the reflection coefficient on a multilayer collector mirror optimized for reflecting radiation at a wavelength of 11.25 nm. The curves measured at the center of the mirror ($r = 0$) and at the edge of the aperture ($r = 20$ mm) are shown.

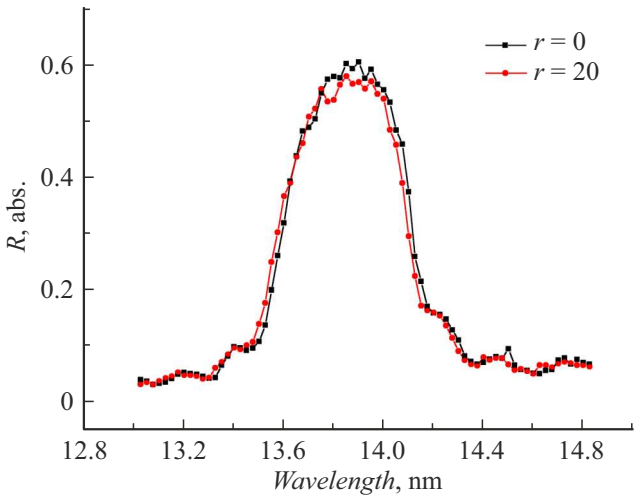

Figure 3. Spectral dependences of the reflection coefficient on a multilayer collector mirror optimized for reflecting radiation at a wavelength of 13.9 nm. The curves measured at the center of the mirror ($r = 0$) and at the edge of the aperture ($r = 20$ mm) are shown.

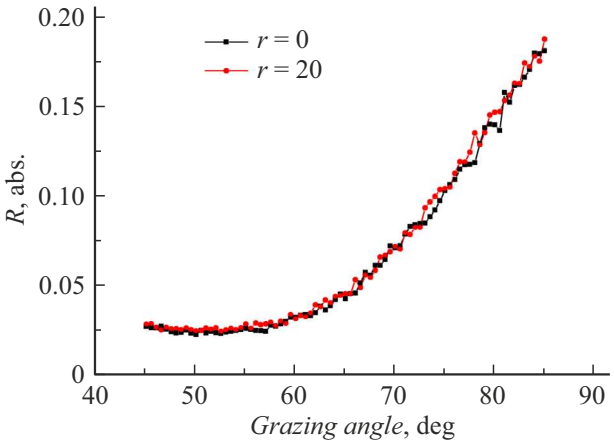

Figure 4. Angular dependences of the reflection coefficient on a multilayer collector mirror optimized for reflecting radiation at a wavelength of 30.4 nm. The curves measured at the center of the mirror ($r = 0$) and at the edge of the aperture ($r = 20$ mm) are shown.

synthesized structure with reference points measured on some characteristic lines using a laboratory reflectometer based on a grating monochromator spectrometer RSM-500 and an X-ray tube as a source [31], as well as a reflectometer with a gas discharge source, are shown in Fig. 5.

The measured transmission coefficients on the characteristic lines of solid-state targets of an X-ray tube and a gas discharge source for a beryllium film with a thickness of $d = 200$ nm, as well as the value obtained in visible light (using He–Ne laser radiation) are presented in Table. 1.

As can be seen, a thin ($d = 200$ nm) beryllium film has high transmission in a wide range of wavelengths from K the absorption edge of beryllium ($\lambda = 11.2$ nm) up to a

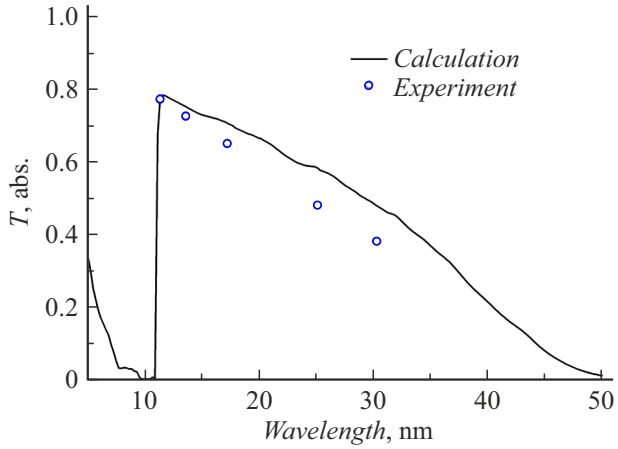

Figure 5. Calculated and experimentally measured spectral dependence of the transmission coefficient of the filter — Be film with thickness of $d = 200$ nm.

Table 1. Transmission coefficients of the Be filter

Wavelength, nm	Transition	Transmittance
11.4	BeK_α	0.772
13.5	SiL_α	0.725
30.4	He II	0.38
633	Ne $(5s \rightarrow 3p)$	$5.6 \cdot 10^{-6}$

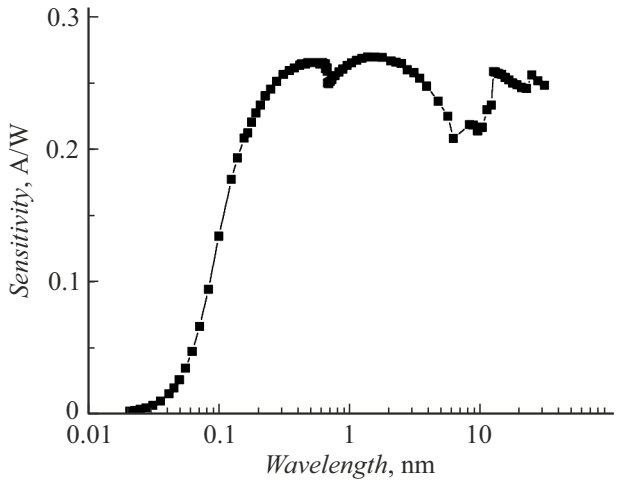

Figure 6. Spectral sensitivity of detector SPD-100UV.

wavelength of about 50 nm, as well as high suppression of longer-wavelength radiation, including visible radiation. The filter is installed directly in front of the sample and allows exposure only of the wavelength resonantly reflected from the multilayer mirror, without affecting the result of the long-wave background.

EUV radiation detector SPD-100UV is installed in place of the sample with a photoresist to control the radiation dose [32]. The spectral dependence of the detector sensitivity, captured on the BESSYII synchrotron (Germany), is shown in Fig. 6.

4. Bench testing

The operating gas Kr and Kr X ion radiation was used for obtaining radiation with a wavelength of 11.2 nm, Ar (ion Ar VIII) was used for obtaining radiation with a wavelength of 13.9 nm, He (ion He II) was used for obtaining radiation with a wavelength of 30.4 nm.

At the preliminary stage of the study, the doses of electromagnetic radiation absorbed by photoresist samples during exposure were estimated. To do this, EUV radiation detector SPD-100UV was installed in the area of the focus spot of the monochromator mirror with an additional block of two filters to suppress parasitic radiation reflected from the walls of the chamber and entering the detector aperture, then the signal registered by the detector was recorded, and the radiation power was estimated based on the signal value. The laser radiation pulse repetition rate and the frequency of synchronized opening of the gas nozzle valve in experiments at wavelengths 13.9 and 30.4 nm was 10 Hz and it was 1 Hz for 11.2 nm.

Here is an example of a calculation for a wavelength of 13.9 nm. The detector, operating in current mode, records a signal after a monochromator mirror optimized for wavelength $\lambda = 13.9$ nm, and a pair of spectral filters. In this case, the diode current was $I_{\text{det}} = 2.2 \cdot 10^{-6}$ A.

$$P_{\text{det}} = I_{\text{det}}/\eta. \tag{1}$$

The sensitivity of the detector at the wavelength of $\lambda = 13.9$ nm is $\eta = 0.25$ A/W. In this case, the radiation power received by the detector:

$$P_{\text{det}} = I_{\text{det}}/\eta = 2.2 \cdot 10^{-6}/0.25 = 8.8 \cdot 10^{-6}\,\text{W}. \tag{2}$$

Taking into account the transmission coefficients of an additional pair of filters, the power transmitted to the exposed sample is

$$P_s = P_{\text{det}}/T_{2f} = 8.8 \cdot 10^{-6}/(0.725 \times 0.725) = 1.6 \cdot 10^{-5}\,\text{W}. \tag{3}$$

It is necessary to determine the size of the focus spot to determine the radiation dose transmitted to the sample. EUV sensitive resist VPR-13 based on PMMA [33] applied to a silicon wafer was used to solve this problem. A plate with a resist was fixed to a linear translator and when the sample was moved, several illumination spots with different exposure times were formed on its surface (Table 2). Then the resist was developed (by dipping into a 20% solution of methyl ethyl ketone in isopropyl alcohol, the time of development was — 1 min) and the spot size was determined using an optical microscope MEIJI MT8530 (Japan) with a graduated motorized table. The spot size for the sample exposed at a wavelength of 13.9 nm was $S = 0.7 \times 1.6$ mm, a photo of the developed sample is shown in Fig. 7, *b*. The oblong shape of the spot is

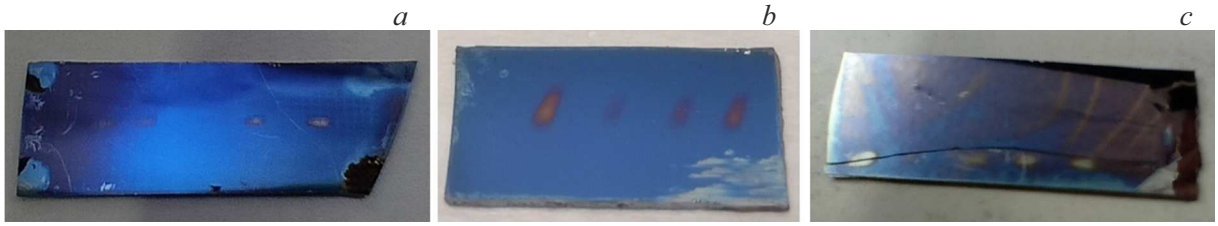

Figure 7. Photo of exposed and developed samples. λ, nm: *a* — 11.2, *b* — 13.9, *c* — 30.4.

Table 2. Exposure dose values for the sample shown in Fig. 7

№areas	Exposure time, s	Dose, mJ/cm^2
1	10	36
2	1	3.6
3	2.5	9
4	5	18

explained by the shape of the laser plasma, extended in the direction of propagation of the laser beam and narrow in the transverse direction. The radiation doses absorbed by the sample during exposure were determined taking into account the size of the spot (Table 2).

Similar measurements were carried out at wavelengths of 11.2 and 30.4 nm. Images of exposed and developed samples are shown in Fig. 7, *a, c*. The spot size for the sample exposed at a wavelength of 11.2 nm was 0.5×1.2 mm, and it was 0.5×1.1 mm for the sample exposed at a wavelength of 30.4 nm. In this case, the signal at the detector was 11.2 nm $I_{\text{det}} = 5.5 \cdot 10^{-6}$ A, and at the wavelength of 30.4 nm — $I_{\text{det}} = 2.5 \cdot 10^{-8}$ A.

The radiation doses received at each exposure point were calculated taking into account the signal at the detector, the sensitivity of the detector, the spot size and the transmission of filters at wavelengths 11.2 and 30.4 nm. The illumination times and the corresponding radiation doses for samples exposed at wavelengths of 11.2 and 30.4 nm are given in Table 3.

The radiation doses for each wavelength per 1 pulse of laser radiation are listed in Table 4.

Thus, the device was tested using the example of EUV radiation-sensitive resist VPR-13, which was previously studied. For all wavelengths (11.2, 13.9 and 30.4 nm), it was possible to register a signal on the detector, obtain illumination spots, measure their size and calculate the radiation dose transmitted to the sample at each illumination spot.

Conclusion

An experimental test bench was developed and assembled for the study of photoresists sensitive to short-wave

Table 3. Exposure dose values for samples shown in Fig. 7, *a, b*

№areas	Exposure time, s	Dose, mJ/cm^2
$\lambda = 11.2$ nm		
1	5	8.1
2	3	4.9
3	2	3.2
4	7	11.3
5	10	16.2
$\lambda = 30.4$ nm		
1	180	27.0
2	30	4.5
3	60	9.0
4	120	18.0
5	150	22.5

Table 4. Radiation dose in spot per 1 laser pulse

Wavelength, nm	Dose, mJ/(cm$^2 \cdot$ imp)
11.2	1.6
13.9	0.36
30.4	0.015

(SXR, EUV, VUV) radiation. The test bench is provided with a laser-plasma source of exposure radiation, and to minimize contamination of the illuminator optics, a laser target in the form of a jet of gas flowing from a pulsed nozzle is used. The source radiation is collected and monochromatized by a spherical collector mirror with a multilayer interference coating, spectral filtration is provided by a thin-film absorption filter with suppression of the long-wave background up to $\sim 6 \cdot 10^{-6}$. The motorized slide table allows testing samples up to 25 mm in length with exposure of several points on one plate during one pumping of the vacuum chamber.

The test bench is provided with a set of mirrors that allows working at three wavelengths: 11.2, 13.9

and 30.4 nm; additional mirrors and spectral filters for other wavelengths can be manufactured as needed. For all available mirrors, the rate of dose set (at pulse repetition rate 1−10 Hz) was studied, determined by the power of the EUV source, the size of the spot on the resist and the characteristics of the „mirror−filter“ pair, which is about 16 mW/cm^2 for $\lambda = 11.2$ nm, 3.6 mW/cm^2 for $\lambda = 13.9$ nm and 0.15 mW/cm^2 for $\lambda = 30.4$ nm.

Funding

The study was supported financially by the Ministry of Science and Higher Education of the Russian Federation (agreement № 075-15-2021-1361).

Conflict of interest

The authors declare that they have no conflict of interest.

References

[1] M.N. Toropov, A.A. Akhsakhalyan, M.V. Zorina, N.N. Salashchenko, N.I. Chkhalo, Yu.M. Tokunov. Tech. Phys., **65** (11), 1873 (2020). DOI: 10.1134/S1063784220110262
[2] M.N. Toropov, A.A. Akhsakhalyan, I.V. Malyshev M.S. Mikhaylenko, A.E. Pestov, N.N. Salaschenko, A.K. Chernyshov, N.I. Chkhalo. Tech. Phys., **92** (13), 2141 (2022). DOI: 10.21883/TP.2022.13.52235.108-21
[3] N.I. Chkhalo, I.V. Malyshev, A.E. Pestov, V.N. Polkovnikov, N.N. Salashchenko, M.N. Toropov, A.A. Soloviev. Appl. Opt., **55** (3), 619 (2016). DOI: 10.1364/AO.55.000619
[4] M. Mastenbroek. Proc. SPIE, **10809**, 1080904 (2018). DOI: 10.1117/12.2502785
[5] A. Zeng. SHS Web Conf., **163**, 03021 (2023). DOI: 10.1051/shsconf/202316303021
[6] A. Pirati, J. van Schoot, K. Troost, R. van Ballegoij, P. Krabbendam, J. Stoeldraijer, E. Loopstra, J. Benschop, J. Finders, H. Meiling, E. van Setten, N. Mika, J. Dredonx, U. Stamm, B. Kneer, B. Thuering, W. Kaiser, T. Heil, S. Migura. Proc. SPIE, **10143**, 101430G-1 (2017). DOI: 10.1117/12.2261079
[7] S.S. Andreev, M. Barysheva, N. Chkhalo, S.A. Gusev, A. Pestov, V.N. Polkovnikov, D.N. Rogachev, N.N. Salashchenko, Yu.A. Vainer, S.Yu. Zuev. Tech. Phys., **55** (8), 1168 (2010). DOI: 10.1134/S1063784210080153
[8] I.A. Kopylets, V.V. Kondratenko, E.N. Zubarev, D.L. Voronov, E.M. Gullikson, E.A. Vishnyakov, E.N. Ragozin. Appl. Surf. Sci., **307**, 360 (2014). DOI: 10.1016/j.apsusc.2014.04.038
[9] S.S. Andreev, M.M. Barysheva, N.I. Chkhalo, S.A. Gusev, A. Pestov, V. Polkovnikov, N. Salashchenko, L. Shmaenok, Y. Vainer, S. Zuev. Nucl. Instrum. Methods Phys. Res. A, **603** (1−2), 80 (2009). DOI: 10.1016/j.nima.2008.12.165
[10] T. Tsarfati, E. Zoethout, E. Louis, R. van de Kruijs, A. Yakshin, St. Müllender, F. Bijkerk. Proc. SPIE, **7271**, 72713V (2009). DOI: 10.1117/12.824434
[11] T. Tsarfati, E. Zoethout, E. Louis, F. Bijkerk. Thin Solid Films, **518** (5), 1365 (2009). DOI: 10.1016/j.tsf.2009.09.073
[12] V. Banine, A. Yakunin, D. Glushkov. Next Generation EUV Lithography: Challenges and Opportunities. Int. Workshop Extreme Ultrav. Sources, T. 24, Dublin (2010).
[13] N.I. Chkhalo, N.N. Salashchenko, AIP Adv., **3** (8), 082130 (2013). DOI: 10.1063/1.4820354
[14] D.G. Volgunov, I.G. Zabrodin, B.A. Zakalov, S.Yu. Zuev, I.A. Kas'kov, E.B. Kluenkov, A.E. Pestov, V.N. Polkovnikov, N.N. Salashchenko, L.A. Suslov,M.N. Toropov, N.I. Chkhalo. Bull. Russ. Acad. Sci.: Phys., **75** (1), 49 (2011). DOI: 10.3103/S1062873811010278
[15] N.I. Chkhalo, V.N. Polkovnikov, N.N. Salashchenko, M.N. Toropov. Proc. SPIE, **10224**, 102241O (2016). DOI: 10.1117/12.2267125
[16] N.I. Chkhalo, V.N. Polkovnikov, N.N. Salashchenko, R.A. Shaposhnikov. Tech. Phys., **67** (8), 1023 (2022). DOI: 10.21883/TP.2022.08.54567.102-22
[17] N.N. Salashchenko, N.I. Chkhalo, N.A. Dyuzhev. J. Surf. Invest.: X-Ray, Synchrotron Neutron Tech., **12** (5), 944 (2018). DOI: 10.1134/S1027451018050324
[18] Electronic media. Available at: https://www.roseltorg.ru/procedure/0173100009523000003
[19] K.C. Johnson. J. Vac. Sci. Technol. B, **30** (5), 051606 (2012). DOI: 10.1116/1.4752112
[20] S.A. Bulgakova, A.Ya. Lopatin, V.I. Luchin et al. Nucl. Instrum. Methods Phys. Res. A, **448** (1−2), 487 (2000). DOI: 10.1016/S0168-9002(00)00237-0
[21] S.A. Bulgakova, A.Ya. Lopatin, V.I. Luchin, L.M. Mazanova, N.N. Salashchenko. Poverkhnost', **1**, 133 (1999) (in Russian).
[22] S.A. Bulgakova, M.M. Johns, E.A. Kiseleva, E.V. Skorokhodov, A. Pestov, A.Ya. Lopatin, S.A. Gusev, V. Luchin, N. Chkhalo, N.N. Salashchenko. Bull. Russ. Acad. Sci.: Phys., **76** (2), 159 (2012). DOI: 10.3103/S1062873812020050
[23] S.A. Bulgakova, M.M. Jons, A.E. Pestov, M.N. Toropov, N. Chkhalo, S.A. Gusev, E.V. Skorokhodov, N.N. Salashchenko. Russ. Microelectron., **42** (3), 165 (2013). DOI: 10.1134/S1063739713020054
[24] E.A. Vishnyakov, K.N. Mednikov, A.A. Pertsov, E.N. Ragozin, A.A. Reva, A. Ulyanov, S. Shestov. Quantum Elec., **39** (5), 474 (2009). DOI: 10.1070/QE2009v039n05ABEH013902
[25] A.Ya. Lopatin, V.I. Luchin, A.N. Nachay, A.A. Perekalov, A.E. Pestov, N.N. Salashchenko, A.A. Soloviev, N.N. Tsybin, N.I. Chkhalo. Tech. Phys., **68** (7), 829 (2023). DOI: 10.61011/TP.2023.07.56623.97-23
[26] N.I. Chkhalo, D.E. Pariev, V.N. Polkovnikov, N.N. Salashchenko, R.A. Shaposhnikov, I.L. Stroulea, M.V. Svechnikov, Yu.A. Vainer, S.Yu. Zuev. Thin Solid Films, **631**, 106 (2017). DOI: 10.1016/j.tsf.2017.04.020
[27] S.A. Garakhin, N.I. Chkhalo, I.A. Kas'kov, A.Ya. Lopatin, I.V. Malyshev, A.N. Nechay, A.E. Pestov, V.N. Polkovnikov, N.N. Salashchenko, M.V. Svechnikov, N.N. Tsybin, I.G. Zabrodin, S.Yu. Zuev. Rev. Sci. Instrum., **91** (6), 063103 (2020). DOI: 10.1063/1.5144489
[28] S.Yu. Zuev, A.V. Mitrofanov. Poverkhnost', **1**, 81 (2002) (in Russian).
[29] E.N. Ragozin, K.N. Mednikov, A.A. Pertsov, A.S. Pirozhkov, A.A. Reva, S. Shestov, A. Ulyanov, E.A. Vishnyakov. Proc. SPIE, **7360**, 73600N (2009). DOI: 10.1117/12.820750
[30] S.V. Kuzin, I.A. Zhitnik, S.V. Shestov, S.A. Bogachev, O.I. Bugaenko, A.P. Ignat'ev, A.A. Pertsov, A.S. Ulyanov, A.A. Reva, V.A. Slemzin, N.K. Sukhodrev, Yu.S. Ivanov, L.A. Goncharov, A.V. Mitrofanov, S.G. Popov, T.A. Shergina, V.A. Solov'ev, S.N. Oparin, A.M. Zykov. Solar System Res, **45** (2), 162 (2011). DOI: 10.1134/S0038094611020110

[31] M.S. Bibishkin, D.P. Chekhonadskih, N.J. Chithalo, E.B. Kluyenkov, A.E. Pestov, N.N. Salashchenko, L.A. Shmaenok, I.G. Zabrodin, S.Yu. Zuev. Proc. SPIE, **5401**, 8 (2004). DOI: 10.1117/12.556949
[32] P.N. Aruev, M.M. Barysheva, B.Ya. Ber, N.V. Zabrodskaya, V.V. Zabrodskii, A.Ya. Lopatin, A.E. Pestov, M.V. Petrenko, V.N. Polkovnikov, N.N. Salashchenko. Quantum Electron., **42** (10), 943 (2012). doi: 10.1070/QE2012v042n10ABEH014901
[33] S.A. Bulgakova, A.Ya. Lopatin, V.I. Luchin et al. Nucl. Instrum. Methods Phys. Res. A, **448** (1−2), 487 (2000). DOI: 10.1016/S0168-9002(00)00237-0

Translated by A.Akhtyamov